elektron ámbar

Original Article

Revista elektron, Vol. 5, No. 2, pp. 100-104 (2021)
https://doi.org/10.37537/rev.elektron.5.2.136.2021

Numerical modeling of radiation-induced charge loss in CMOS floating gate cells

Modelización numérica de la pérdida de carga inducida por radiación en celdas CMOS de puerta flotante

L. Sambuco Salomone [#1], M. A. Garcia-Inza [#], S. Carbonetto [#], A. Faigón [#]

[#] *Laboratorio de Física de Dispositivos - Microelectrónica, INTECIN, Facultad de Ingeniería, Universidad de Buenos Aires - CONICET*
Av. Paseo Colón 850, CABA, Argentina
[1] lsambuco@fi.uba.ar

Recibido: 07/10/21; Aceptado: 04/11/21

***Abstract*—The radiation response of programmed/erased floating gate cells is studied by numerical simulations through a recently developed physics-based numerical model. The role played by oxide trapped charge in the overall threshold voltage shift with dose is properly evaluated by varying the capture rate of radiation-generated holes. A simplified analytical model is considered, and its limitations are discussed.**

Keywords: radiation effects; floating gate cells; numerical modeling.

***Resumen*—Mediante un modelo numérico desarrollado recientemente y basado en principios físicos, se estudia la respuesta a la radiación de celdas de compuerta flotante programadas/borradas. El rol que juega la captura de carga en los óxidos en el desplazamiento total de la tensión umbral con la dosis es debidamente evaluado a través de la variación de la tasa de captura de los huecos generados por radiación. Se considera un modelo analítico simplificado y se discuten sus limitaciones.**

Palabras clave: efectos de radiación; celdas de puerta flotante; modelización numérica.

I. INTRODUCTION

Floating gate (FG) cells are conventional metal-oxide-semiconductor field-effect transistors (MOSFETs) with the addition of a polysilicon layer embedded in the gate oxide, between the control gate and the silicon substrate. The device is schematically shown in Fig. 1. As the floating gate is electrically isolated, it serves as a charge storage layer, making the whole structure a nonvolatile memory. The charge at the floating gate can be manipulated by carrier injection through the thin oxide layer between the floating gate and the channel, known as the tunnel oxide. The control gate usually aids this process and also is used to read the state of the cell. Due to their high density, small power consumption, and large program/erase cycling endurance, floating gate cells are the standard devices for nonvolatile memory applications. However, they are known to be sensitive to ionizing radiation, either due to the peripheral circuitry [2]-[3], or to the loss of the charge stored in the FG, ultimately leading to bit errors, as observed in planar [4]-[5], and in novel 3D technologies [6]. On the other hand, this radiation sensitivity can be seized, so different floating gate-based dosimeters were proposed [7]-[13]. One of the advantages of a FG cell compared to a conventional MOS dosimeter is that the charge preinjected into the floating gate generates the necessary oxide electric field to increase the effective radiation-induced electron-hole pair generation, making it possible to achieve a good sensitivity even if the sensor is unbiased during irradiation [8].

Either to mitigate radiation effects to employ FG cells in space environments, or to exploit them for dosimetry purposes, it is mandatory to have a physical model that deals with radiation-induced floating gate charge loss in a programmed/erase cell. Snyder et al. [14], proposed an analytical model for the dose evolution of the threshold voltage, based on the main mechanisms responsible for the floating gate charge loss. This model was later extended to modern technologies by other authors [15]-[16]. However, the predictive capability of this model was disputed [17], so that more accurate physics-based models are needed to reproduce and predict the response of FG cells exposed to ionizing radiation. For that purpose, we developed a physics-based numerical model that self-consistently solves the set of equations describing total dose effects in FG cells [18].

The aim of this work is twofold: for one hand we explore what a physics-based numerical model can unveil regarding the role played by charges trapped in both oxides during the exposure to radiation of a programmed/erased FG cell, and on the other hand we compare it with the Snyder model.

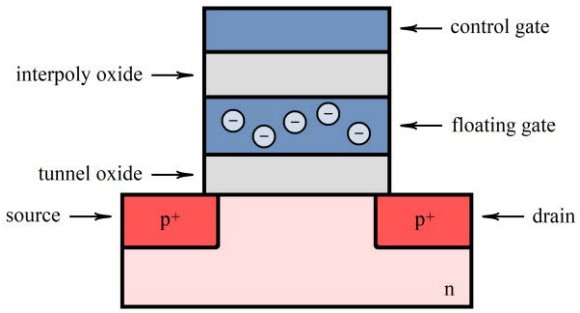

Fig. 1. Schematic representation of a floating gate p-channel transistor.

II. THEORY

A. Physics-based numerical model

Figure 2 summarizes the main physical processes that take place when a programmed cell is exposed to ionizing radiation. Next, we briefly describe how the model works.

For more details about modeling of total dose effects in MOS oxides, the reader can refer to [19]-[21].

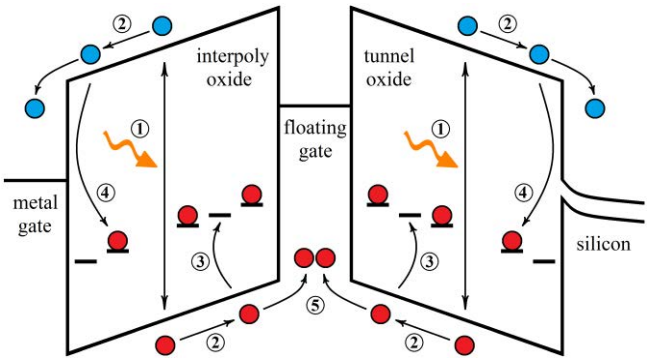

Fig. 2. Band diagram schematic representation of the physical model for a floating gate structure with zero applied bias and negative charge initially at the floating gate. ① charge generation and initial recombination, ② electron (blue) and hole (red) transport, ③ hole trapping, ④ trapped hole neutralization through electron trapping, and ⑤ charge injection into the floating gate.

Radiation generates electron-hole pairs within both oxides, a fraction of which escapes from initial recombination. Remaining carriers move drifted by the electric field. Once a hole is within a small radius around an oxygen vacancy, there is a probability for it to be trapped there. Electron capture at a positive charged defect leads to trapped hole neutralization. Charge in the floating gate varies according to the injection of carriers from both oxides. The system of equations to be solved is the following,

$$\frac{dF}{dx} = -\frac{q}{\varepsilon_{ox}}\left(p_t + p_f - n_f\right) \tag{1}$$

$$\frac{dn_f}{dt} = -\frac{dj_n}{dx} + R_g - R_n n_f p_t \tag{2}$$

$$\frac{dp_f}{dt} = -\frac{dj_p}{dx} + R_g - R_c p_f \left(P_t - p_t\right) \tag{3}$$

$$\frac{dp_t}{dt} = R_c p_f \left(P_t - p_t\right) - R_n n_f p_t \tag{4}$$

$$\frac{dp_{fg}}{dt} = j_{p,fg} - j_{n,fg} \tag{5}$$

where n_f and p_f are the densities of free electrons and holes, respectively, p_t is the density of trapped holes, P_t is the density of traps, p_{fg} is the carrier density at the floating gate, R_c and R_n are the trapping and neutralization rates, respectively. The generation rate is $R_g = g_0 Y D_r$, where $g_0 = 8.1\times10^{14}$ cm^{-3}Gy^{-1}, Y is the fractional yield, and D_r is the dose rate. x is referred to the Si/SiO$_2$ interface. F is the electric field, q is the elementary charge and ε_{ox} is the SiO$_2$ permitivity ($3.9\varepsilon_0$). The electron (j_n) and hole (j_p) fluxes are described by the usual drift-diffusion model. $j_{n,fg}$ and $j_{p,fg}$ are the electron and hole fluxes across both oxide/floating gate interfaces, respectively.

The V_t-shift due to charge in the oxides and the floating gate is calculated using,

$$\Delta V_t = -\frac{q}{\varepsilon_{ox}}\left[\int_0^{t_{to}+t_{ip}} p_t\left(t_{to}+t_{ip}-x\right)dx + p_{fg}t_{ip}\right] \tag{6}$$

where t_{to} and t_{ip} are the tunnel and interpoly oxides thicknesses, respectively. Free carriers were neglected due to their much lower concentrations relative to the trapped charge.

B. Snyder model

In 1989, Snyder et al. [14] presented a simplified model for the discharge of floating gate cells during irradiation. This model is based on the same physics previously described with the addition of photoemission of carriers from the floating gate into the oxides. However, the distinctive feature of the Snyder model depends on the following two assumptions: (i) holes are trapped within the oxides close to the corresponding FG/SiO$_2$ interface, and (ii) fractional yield depends linearly on electric field, which allow to reduce the V_t evolution with dose to the following first order expression,

$$\Delta V_t = \Delta V_{t0} \exp\left(-D/D_0\right) \tag{7}$$

where D is the absorbed dose, and ΔV_{t0} and D_0 are the fitting parameters representing the total V_t-shift and a characteristic dose, respectively.

III. Results and Discussion

The floating gate devices considered in simulations are p-channel MOSFETs from a 1.5 µm complementary MOS (CMOS) process. The thickness of the tunnel and interpoly oxides are t_{to} = 30 nm and t_{ip} = 57 nm, respectively. Also, we assume γ-irradiation. For other irradiation source, the expression for the electric field dependence of the fractional yield must be modified.

Simulations of the radiation response of FG cells with different initial V_t values, corresponding to different initial charge at the floating gate, were performed. As a first case, we considered a capture rate $R_c = 10^{-14}$ cm^{3}s^{-1}, low enough for the oxide trapped holes contribution to be non-relevant, so the dynamic is dominated by the injection of carriers into the floating gate. Neutralization rate was $R_n = 10^{-6}$ cm^{3}s^{-1}, although the response is almost independent of it, given the low value of R_c. The results are shown in Fig. 3. The V_t vs. dose curves are consistent with the progressive loss of the charge stored at the floating gate with the device reaching a final V_t value independent of the initial condition and corresponding to the cell with minimal amount of stored charge. Also, each curve was fitted with Snyder model expression (7). As the initial charge at the floating gate increases, the first order fit is worse, tending to overestimate the discharge for low dose, whereas the opposite occurs for high dose. Particularly relevant is the analysis of the characteristic dose D_0 needed to reproduce the results. First, it is observed that D_0 is independent of whether the initial charge in the floating gate is positive or negative, which is expected because of the low R_c value that leads to responses dominated by the injection in the floating gate of carriers generated in both oxides. Second, D_0 increases with the magnitude of this initial charge. This result is consistent with previously reported results [17], and differs with the assumption made by Snyder model about D_0 depending only on external bias. Physically, this result can be explained because of the sublinear dependence of the fractional yield on electric field. In other terms, the amount

of charge needed to restore the device to the chargeless condition is equal to the initial charge at the floating gate p_{fg0}. As p_{fg0} increases, the electric field in both oxides increases and a higher fraction of electron-hole pairs escape from the initial recombination, but as this yield is not strictly linear with electric field, more dose is needed to generate the amount of charge that compensates for the excess of electrons in the floating gate.

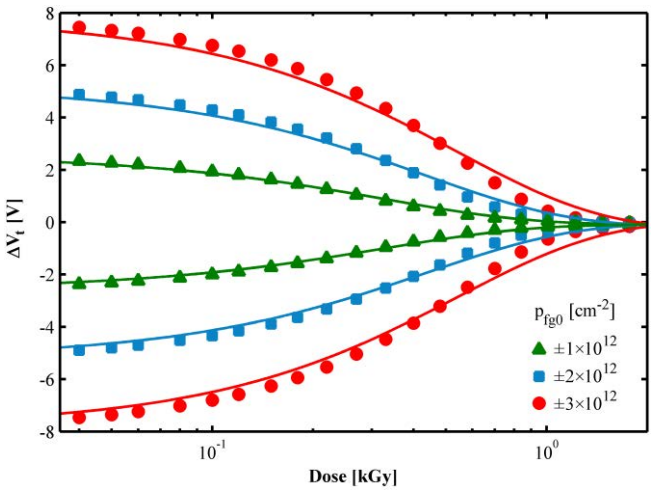

Fig. 3. Numerical simulations (symbols) and Snyder's first order fits (lines) of the floating gate charge loss for different initial conditions and $R_c = 10^{-14}$ cm^{3}s^{-1}, and $R_n = 10^{-6}$ cm^{3}s^{-1}. Characteristic dose values D_0 are 326 Gy for $p_{fg0} = \pm 1\times10^{12}$ cm^{-2}, 433 Gy for $p_{fg0} = \pm 2\times10^{12}$ cm^{-2}, and 539 Gy for $p_{fg0} = \pm 3\times10^{12}$ cm^{-2}.

To evaluate the impact that hole trapping within the oxides has on the response, simulations were made with an initial charge $p_{fg0} = \pm 2\times10^{12}$ cm^{-2}, neutralization rate $R_n = 10^{-6}$ cm^{3}s^{-1}, and two values for the capture rate R_c. The results are shown in Fig. 4. As observed, when $R_c = 10^{-12}$ cm^{3}s^{-1} the steady state V_t value differs from the one corresponding to a completely discharged cell, but it is shifted towards negative voltages due to the holes trapped in both oxides. Again, the Snyder expression (7) was used to fit the curves, failing to reproduce the long-term behaviour of the curves with the higher R_c value, especially when the floating gate is initially filled with electrons. Also, when hole capture becomes relevant, the characteristic dose D_0 starts to depend on whether the cell is initially programmed or erased.

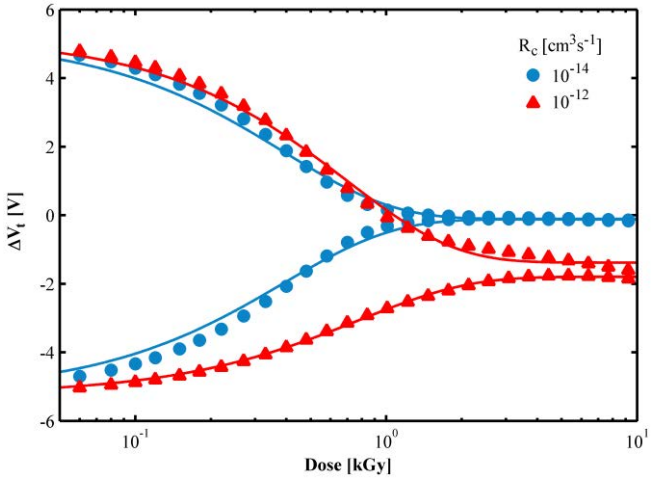

Fig. 4. Numerical simulations (symbols) and Snyder first order fits (lines) of the floating gate charge loss for $p_{fg0} = \pm 2\times10^{-12}$ cm^{-2}, $R_n = 10^{-6}$ cm^{3}s^{-1}, and different R_c values.

To get some insight about the microscopic processes involved in the radiation response, Fig. 5 shows the ΔV_t contributions due to the charge at the floating gate ($\Delta V_{t(fg)}$), and holes trapped in tunnel ($\Delta V_{t(to)}$) and interpoly ($\Delta V_{t(ip)}$) oxides for the two simulations of Fig. 4 that start with a programmed cell ($p_{fg0} = -2\times10^{12}$ cm^{-2}). For a low capture rate, the response is dominated by the variation of the charge at the floating gate, whereas for the higher capture rate value, it is observed that the hole trapping within the oxides does not allow the floating gate to be totally discharged. Not only a remnant of the electrons initially at the floating gate remain there at the end of the irradiation, but also the trend in the change can even turn around and the density of electrons at the floating gate increases slightly for high doses. As the final V_t value is lower than that for a device without charge, the contribution of holes trapped in both oxides overcompensate the electrons in the floating gate. It is worth to notice that the ΔV_t contribution due to holes trapped within the interpoly oxide is not monotone.

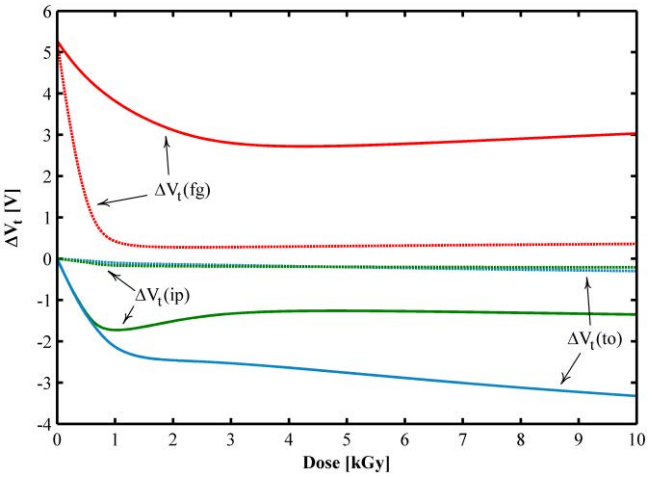

Fig. 5. Contributions to the overall ΔV_t due to charges at the floating gate and trapped in both oxides from the simulations of Fig. 4 that start with $p_{fg0} = -2\times10^{-12}$ cm^{-2}. Solid lines correspond to $R_c = 10^{-12}$ cm^{3}s^{-1}, and dashed lines correspond to $R_c = 10^{-14}$ cm^{3}s^{-1}. In both cases, $R_n = 10^{-6}$ cm^{3}s^{-1}.

Figure 6 shows the conduction band electronic energy across the structure for different accumulated dose during the irradiation of a floating gate cell with an initial charge $p_{fg0} = -2\times10^{12}$ cm^{-2}, and physical parameters $R_c = 10^{-12}$ cm^{3}s^{-1} and $R_n = 10^{-6}$ cm^{3}s^{-1}. The spatial distributions of trapped holes in both oxides are shown in Fig. 7. Due to the electric fields in each oxide, holes tend to be accumulated towards the corresponding interfaces with the floating gate. As accumulated dose increases and V_t approaches saturation, the electric field vanishes in each oxide leading to a charge redistribution process that narrows the spatial distribution of trapped holes towards the interfaces.

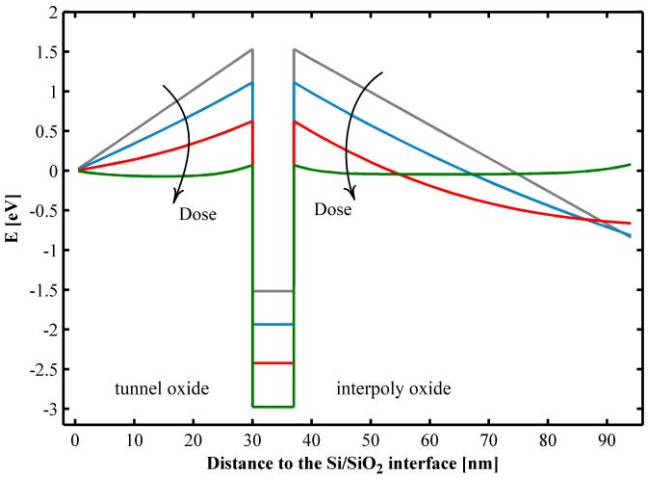

Fig. 6. Conduction band electronic energy as a function of distance for the simulation of floating gate charge loss with $p_{fg0} = -2\times10^{-12}$ cm^{-2}, $R_c = 10^{-12}$ cm^{3}s^{-1} and $R_n = 10^{-6}$ cm^{3}s^{-1} from Fig. 4.

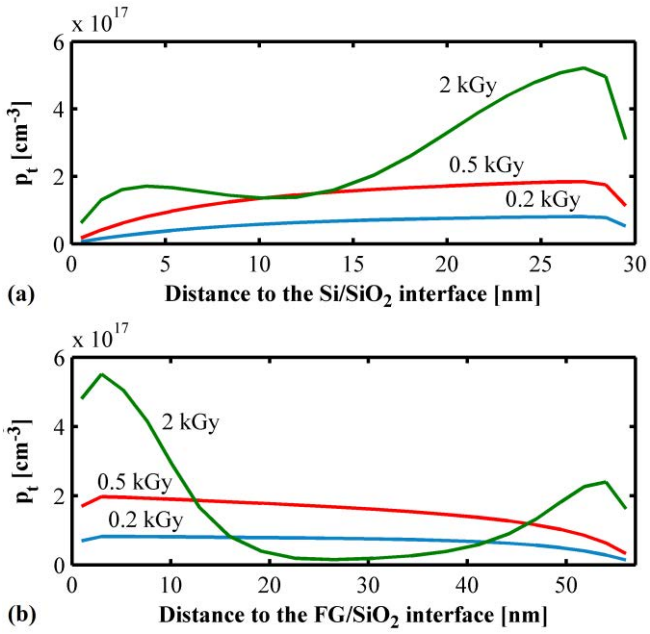

Fig. 7. Spatial distribution of trapped holes within (a) tunnel, and (b) interpoly oxides, for different accumulated doses for the simulation of floating gate charge loss with $p_{fg0} = -2\times10^{-12}$ cm^{-2}, $R_c = 10^{-12}$ cm^{3}s^{-1} and $R_n = 10^{-6}$ cm^{3}s^{-1} from Fig. 4.

IV. Conclusions

The charge loss of programmed/erased floating gate cells due to ionizing radiation exposure at zero bias was studied by means of numerical simulations with a recently developed physics-based model. Once the initial charge at the floating gate and capture and neutralization rates for oxide traps are determined, the model predicts the dose evolution of threshold voltage. Changing the capture rate within the usual range reported in the literature showed that the presence of oxide charges may become relevant, shifting the long-term threshold voltage from its value for a non-charged structure.

Numerical simulations were compared with the Snyder model, which is based on a first order expression for the relation between threshold voltage and absorbed dose. Both models agree on the overall response. Nevertheless, for large initial charge at the floating gate and/or for a moderately high capture rate, the numerically simulated responses departed from this simplified dose dependence. Further comparison with experimental data will help to conclude about the usefulness of both models.

In the future, we intend to extend the model to include other floating gate structures, such as: (i) an oxide-nitride-oxide (ONO) interpoly oxide [15]-[17], (ii) a trap-rich dielectric as trapping layer, as in silicon-oxide-nitride-oxide-silicon (SONOS) charge trapping memories [22]-[23], and (iii) a floating gate that extends over a field oxide for increasing sensitivity in dosimetry applications [7].

Acknowledgment

This work was supported by grants UBACYT 20020190200002BA and 20020170100685BA.

References

[1] S. Gerardin, M. Bagatin, A. Paccagnella, K. Grürmann, F. Gliem, T. R. Oldham, F. Irom, and D. N. Nguyen, "Radiation effects in Flash memories," *IEEE Transactions on Nuclear Science*, vol. 60, no. 3, pp. 1953-1969, 2013.

[2] D. N. Nguyen, S. M. Guertin, G. M. Swift, and A. H. Johnston, "Radiation effects on advanced Flash memories," *IEEE Transactions on Nuclear Science*, vol. 46, no. 6, pp. 1744-1750, 1999.

[3] D. Krawzsenek, P. Hsu, H. Anthony, and C. Land, "Single event effects and total ionizing dose results of a low voltage EEPROM," in *Proc. 2000 IEEE Radiation Effects Data Workshop*, pp. 64-67.

[4] T. R. Oldham, D. Chen, M. R. Friendlich, and K. A. LaBel, "Retention characteristics of commercial NAND Flash memory after radiation exposure," *IEEE Transactions on Nuclear Science*, vol. 59, no. 6, pp. 3011-3015, 2012.

[5] S. Gerardin, M. Bagatin, A. Bertoldo, A. Paccagnella, and V. Ferlet-Cavrois, "Sample-to-sample variability of floating gate errors due to total ionizing dose," *IEEE Transactions on Nuclear Science*, vol. 62, no. 6, pp. 2511-2516, 2015.

[6] M. Bagatin, S. Gerardin, A. Paccagnella, S. Beltrami, A. Costantino, M. Muschitiello, A. Zadeh, and V. Ferlet-Cavrois, "Total ionizing dose effects in 3D NAND Flash memories," *IEEE Transactions on Nuclear Science*, vol. 66, no. 1, pp. 48-53, 2019.

[7] N. G. Tarr, G. F. Mackay, K. Shortt, and I. Thomson, "A floating gate MOSFET dosimeter requiring no external bias supply," *IEEE Transactions on Nuclear Science*, vol. 45, no. 3, pp. 1470-1474, 1998.

[8] N. G. Tarr, K. Shortt, Y. Wang, and I. Thomson, "A sensitive, temperature-compensated, zero-bias floating gate MOSFET dosimeter," *IEEE Transactions on Nuclear Science*, vol. 51, no. 3, pp. 1277-1282, 2004.

[9] M. García Inza, J. Lipovetzky, E. G. Redin, S. Carbonetto, and A. Faigón, "Floating gate pMOS dosimeters under bias controlled cycled measurement," *IEEE Transactions on Nuclear Science*, vol. 58, no. 3, pp. 808-812, 2011.

[10] P. J. McNulty, and K. F. Poole, "Increasing the sensitivity of FGMOS dosimeters by reading at higher temperature," *IEEE Transactions on Nuclear Science*, vol. 59, no. 4, pp. 1113-1116, 2012.

[11] E. García Moreno, E. Isern, M. Roca, R. Picos, J. Font, J. Cesari, and A. Pineda, "Temperature compensated floating gate MOS radiation sensor with current output," *IEEE Transactions on Nuclear Science*, vol. 60, no. 5, pp. 4026-4030, 2013.

[12] M. Álvarez, C. Hernando, J. Cesari, A. Pineda, and E. García Moreno, "Total ionizing dose characterization of a prototype floating gate MOSFET dosimeter for space applications," *IEEE Transactions on Nuclear Science*, vol. 60, no. 6, pp. 4281-4288, 2013.

[13] E.G. Villani, M. Crepaldi, D. DeMarchi, A. Gabrielli, A. Khan, E. Pikhay, Y. Roizin, A. Rosenfeld, and Z. Zhang, "A monolithic 180 nm CMOS dosimeter for wireless in vivo dosimetry," *Radiation Measurements*, vol. 84, pp. 55-64, 2016.

[14] E. S. Snyder, P. J. McWhorter, T. A. Dellin, and J. D. Sweetman, "Radiation response of floating gate EEPROM memory cells," *IEEE Transactions on Nuclear Science*, vol. 36, no. 6, pp. 2131-2139, 1989.

[15] G. Cellere, A. Paccagnella, A. Visconti, M. Bonanomi, P. Caprara, and S. Lora, "A model for TID effects on floating gate memory cells," *IEEE Transactions on Nuclear Science*, vol. 51, no. 6, pp. 3753-3758, 2004.

[16] J. J. Wang, S. Samiee, H.-S. Chen, C.-K. Huang, M. Cheung, J. Borillo, S.-N. Sun, B. Cronquist, and J. McCollum, "Total ionizing dose effects on Flash-based field programmable gate array," *IEEE Transactions on Nuclear Science*, vol. 51, no. 6, pp. 3759-3766, 2004.

[17] J. J. Wang, G. Kuganesan, N. Charest, and B. Cronquist, "Biased-irradiation characteristics of the floating gate switch in FPGA," *IEEE Radiation Effects Data Workshop 2006*, p. 101-104, 2006.

[18] L. Sambuco Salomone, M. Garcia-Inza, S. Carbonetto, J. Lipovetzky, E. Redin, and A. Faigón, "A physics-based model of total ionizing dose effects on floating gate cells," *submitted for publication*.

[19] L. Sambuco Salomone, A. Faigón, and E. G. Redin, "Numerical modeling of MOS dosimeters under switched bias irradiations," *IEEE Transactions on Nuclear Science*, vol. 62, no. 4, pp. 1665-1673, 2015.

[20] L. Sambuco Salomone, A. Holmes-Siedle, and A. Faigón, "Long term effects of charge redistribution in cycled bias operating MOS dosimeter," *IEEE Transactions on Nuclear Science*, vol. 63, no. 6, pp. 2997-3002, 2016.

[21] M. V. Cassani, L. Sambuco Salomone, S. Carbonetto, A. Faigón, E. Redin, and M. Garcia-Inza, "Experimental characterization and numerical modeling of total ionizing dose effects on field oxide MOS dosimeters," *Radiation Physics and Chemistry*, vol. 182, 109338, 2021.

[22] M. Li, J. S. Bi, Y. N. Xu, B. Li, K. Xi, H. B. Wang, J. Liu, J. Li, L. L. Ji, L. Luo, and M. Liu, "Total ionizing dose effects of 55-nm silicon-oxide-nitride-oxide-silicon charge trapping memory in pulse and DC modes," *Chinese Physics Letters*, vol. 35, no. 7, 078502, 2018.

[23] J. S. Bi, Y. N. Xu, G. B. Xu, H. B. Wang, L. Chen, and M. Liu, "Total ionizing dose effects on charge-trapping memory with $Al_2O_3/HfO_2/Al_2O_3$ trilayer structure," *IEEE Transactions on Nuclear Science*, vol. 65, no. 1, pp. 200-205, 2018.